AD-A077 023 BOSTON UNIV MASS DEPT OF ASTRONOMY F/G 4/1
DMSP AURORAL IMAGES AND THE GOOSE BAY IONOSPHERE.(U)
JAN 79 C C CHACKO , M MENDILLO F19628-78-C-0011
UNCLASSIFIED AFGL-TR-79-0023 NL

| OF |
AD
A077023

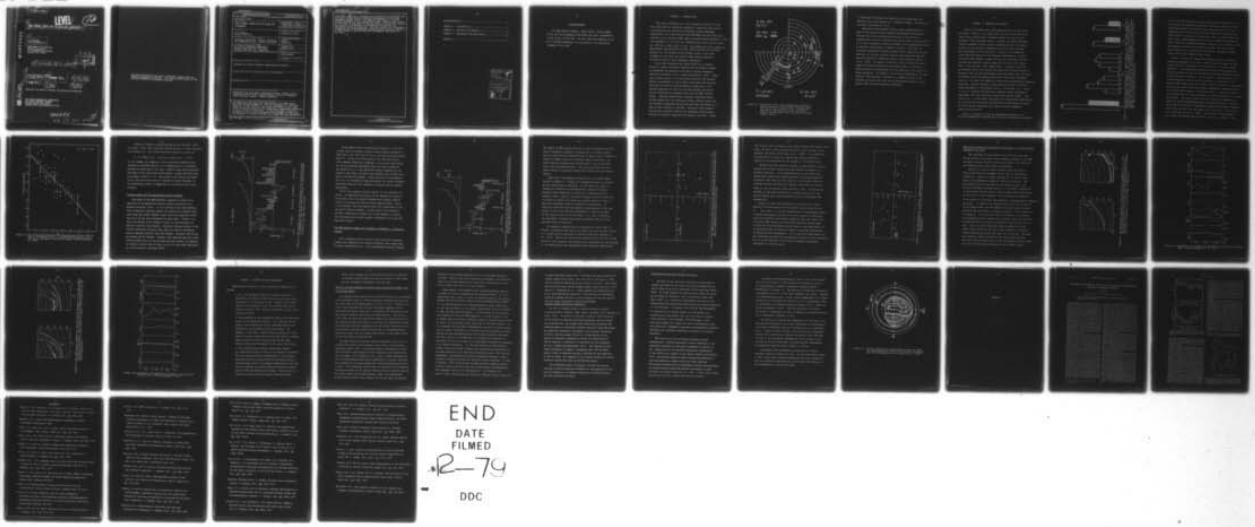

END
DATE
FILMED
12-79
DDC

AD A077023

AFGL-TR-79-0023

LEVEL II

DMSP AURORAL IMAGES AND THE GOOSE BAY IONOSPHERE

C.C. Chacko
Michael Mendillo

Department of Astronomy
Boston University
725 Commonwealth Avenue
Boston, MA 02215

DDC
RECEIVED
NOV 21 1979
E

F19628-78-C-0011

Final Scientific Report,
1 October 1977 — 30 September 1978

January 1979

4643

44

06

Approved for public release; distribution unlimitted

DDC FILE COPY

AIR FORCE GEOPHYSICS LABORATORY
AIR FORCE SYSTEMS COMMAND
UNITED STATES AIR FORCE
HANSCOM AFB, MASSACHUSETTS 01730

406311

79 11 19 135

Qualified requestors may obtain additional copies from the Defense Documentation Center. All others should apply to the National Technical Information Service.

unclassified

SECURITY CLASSIFICATION OF THIS PAGE (When Data Entered)

REPORT DOCUMENTATION PAGE		READ INSTRUCTIONS BEFORE COMPLETING FORM
1. REPORT NUMBER AFGL-TR-79-0023	2. GOVT ACCESSION NO.	3. RECIPIENT'S CATALOG NUMBER
4. TITLE (and Subtitle) DMSP AURORAL IMAGES AND THE GOOSE BAY IONOSPHERE		5. TYPE OF REPORT & PERIOD COVERED Scientific - Final 1 Oct 1977-30 Sep 1978 6. PERFORMING ORG. REPORT NUMBER
7. AUTHOR(s) C.C. Chacko Michael Mendillo		8. CONTRACT OR GRANT NUMBER(s) F19628-78-C-0011
9. PERFORMING ORGANIZATION NAME AND ADDRESS Astronomy Department, Boston University 725 Commonwealth Ave., Boston, MA 02215		10. PROGRAM ELEMENT, PROJECT, TASK AREA & WORK UNIT NUMBERS 62101F 464306 AA
11. CONTROLLING OFFICE NAME AND ADDRESS Air Force Geophysics Laboratory Hanscom AFB, Bedford, MA 01731 Contract Monitor: E.J. Weber/PHI		12. REPORT DATE January 1979 13. NUMBER OF PAGES 44
14. MONITORING AGENCY NAME & ADDRESS (if different from Controlling Office)		15. SECURITY CLASS. (of this report) Unclassified 15a. DECLASSIFICATION/DOWNGRADING SCHEDULE

16. DISTRIBUTION STATEMENT (of this Report)

Approved for public release; distribution unlimited

17. DISTRIBUTION STATEMENT (of the abstract entered in Block 20, if different from Report)

18. SUPPLEMENTARY NOTES

19. KEY WORDS (Continue on reverse side if necessary and identify by block number)

DMSP/Goose Bay Data Base, Continuous Aurora, Diffuse Aurora, Feldstein Auroral Oval, Substorm Phase, Critical Frequency, Total Electron Content, Plasma Convection

20. ABSTRACT (Continue on reverse side if necessary and identify by block number)

The DMSP/Goose Bay data base consisting of all DMSP images obtained between December 9, 1971 and September 21, 1973 with Goose Bay in the field of view forms the basis of this study aimed at examining auroral and ionospheric conditions prevailing in the vicinity of Goose Bay. It was found that little of a systematic nature could be deduced from attempts to correlate the presence of auroral activity near Goose Bay with parameters

DD FORM 1 JAN 73 1473 EDITION OF 1 NOV 65 IS OBSOLETE

unclassified

SECURITY CLASSIFICATION OF THIS PAGE (When Data Entered)

like ΔfoF2, ΔTEC etc., although past studies had established that aurorally induced electron density enhancements in the upper ionosphere always occur a few degrees equatorward of the low latitude boundary of the continuous aurora. Another major result of the study is the finding that the phase of the auroral electrojet activity is important in determining the proximity of continuous aurora to Goose Bay. Two case studies are discussed to illustrate the correspondences between auroral activity captured on DMSP images on the one hand and ionospheric parameters on the other.

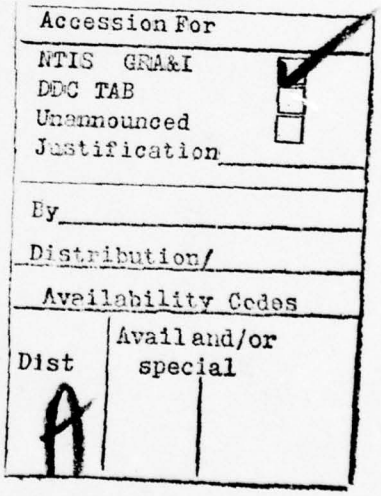

ACKNOWLEDGEMENT

We thank Captain Edward J. Weber and Mr. Jurgen Buchau of the Air Force Geophysics Laboratory for their co-operation in the course of this work. We also thank Ken Schatten of the B.U. Astronomy Department for assistance in the statistical treatment of the data.

CHAPTER 1. INTRODUCTION

This report describes the final scientific results of a one year study aimed at examining ionospheric conditions that prevail in conjunction with optically discernible auroral phenomena. Specifically, the study utilizes the DMSP/Goose Bay data base which consists of all available DMSP images recorded between December 9, 1971 and September 21, 1973 with the ionosphere-monitoring station Goose Bay (65° CGL) in the field of view. The images have been gridded and photographic reproductions with the 100-km overlay are available. However, for the purposes of the present study it was found necessary to work with the original DMSP images themselves archived at the Air Force Geophysics Laboratory.

This study represents the latest effort in an ongoing program at Boston University dealing with the general problem of morphology and dynamics of the high latitude ionosphere [Mendillo and Chacko, 1977; Chacko and Mendillo, 1977]. These past studies showed, on a statistical basis,that the electron density enhancements in the F-region associated with the poleward wall of the main electron density trough occur a few degrees equatorward of the low latitude boundary of diffuse auroral emissions as determined from ISIS and DMSP auroral images. Detailed examinations of several individual events further showed that the separation between diffuse aurora and the poleward trough wall varied from less than one degree to as much as seven degrees in latitude. Moreover, these studies consistently revealed a lack of any systematic relationships between the observed separation and magnetic activity. Figure

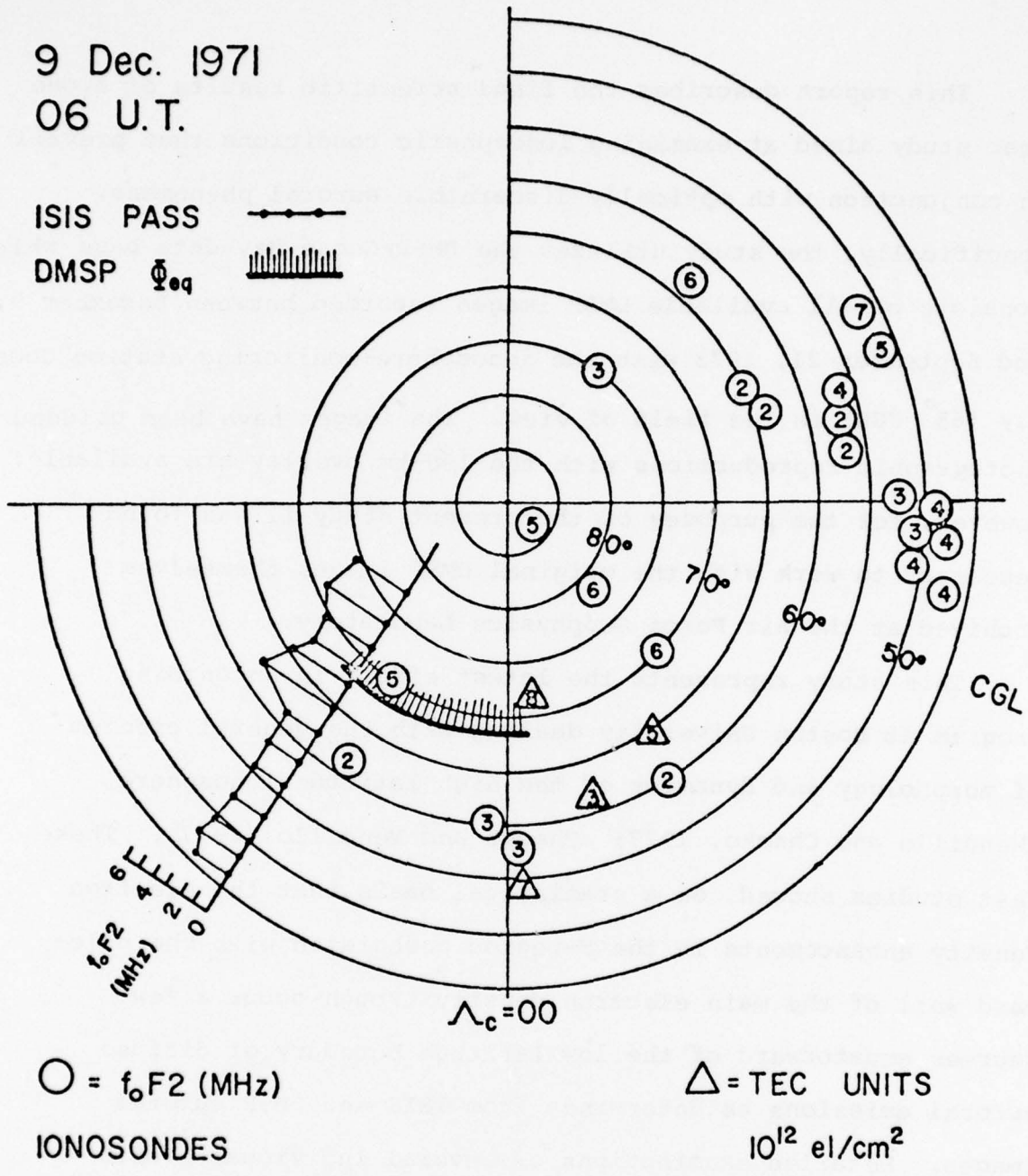

FIGURE 1.1 North polar view in CGL showing the location of near-simultaneous ISIS and DMSP satellite data for 0600 UT on 9 December 1971. Ground-based foF2 values and TEC data at 0600 UT from a network of ionosondes also are presented using integer values.

1, reproduced from Chacko and Mendillo [1977] illustrates the observed inter-relationships in a graphical scheme. [For details see Chacko and Mendillo, 1977].

The picture that emerges from the above considerations is that of the topside electron density enhancements occuring not directly above the instantaneous location of the particle precipitation region as inferred from optical data, but equatorward of it, the latitudinal separation between the two phenomena showing no apparent relationship to magnetic activity. Note that an analogous displacement between visible auroral forms and the poleward wall of the main electron density trough has been observed using the Chatanika incoherent scatter radar technique [Bates, et al., 1973]. We present in Chapter 2 results from the current study that further underscore the general lack of coincidence between particle precipitation and its signature in the night side upper ionosphere. In Chapter 3 we discuss an explanation for this finding. The appendix is devoted to a companion study of the behavior of the F2 peak along the noon-midnight meridian in mid-winter under very quiet magnetic conditions.

CHAPTER 2. ANALYSIS AND RESULTS

Figure 2.1 presents four histograms pertaining to the available data. Figure 2.1 (a) shows that only 136 of the 260 auroral images have yielded useful information about the low latitude boundary of the continuous aurora. Presence of bright moonlight, detector problems, various scaling uncertainties and the unavailability of the original transparencies at the time of scaling have contributed to this situation. Figure 2.1 (b) shows the local time distribution of the available measurements. In what follows we have adopted a simple division of these data into pre-midnight and midnight sectors, comprising the local time ranges 1800 - 2200 and 2200 - 0200 respectively. In general, data for the midnight sector are derived from passes that occurred prior to November, 1972 and the pre-midnight data from passes that took place afterwards, with some overlap occurring in the month of November. Figure 2.1 (c) shows the number of more-or-less simultaneously obtained Goose Bay critical frequency values against scalings of auroral images available in the midnight sector. (See Figure 2.5). Figure 2.1 (d) is a similar histogram that compares another ionospheric observable, the total electron content, with auroral images. (See Figure 2.6). In both these cases pairs of uncoordinated observations are involved and the paucity of simultaneous observations is caused by active auroral conditions that render routine ionospheric observations difficult.

The Q = 0 auroral oval has an equatorward boundary at 70° Corrected Geomagnetic Latitude (CGL) near local midnight and migrates

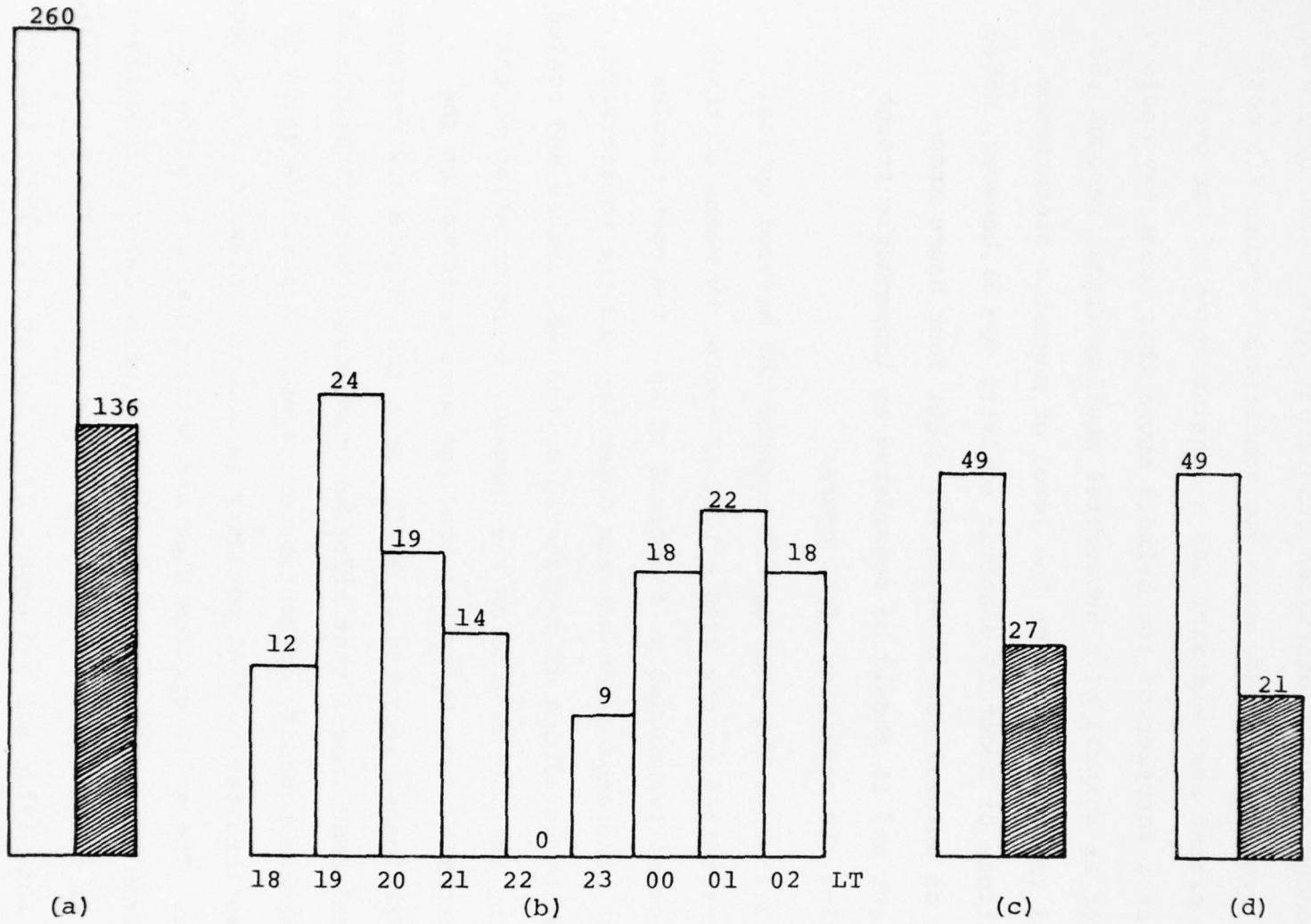

Figure 2.1 Histograms show the distribution of auroral images. (a), Total number of DMSP/Goose Bay auroral images from December 9, 1971 to September 21, 1973 and the number of available scalings. (b), Distribution of available scalings in local time. (For example, there are 12 scalings in the 1800-1900 LT segment). (c), There are 49 DMSP scalings in the 2200-0200 LT sector and 27 simultaneously obtained ΔfoF2 values. (d), Same as (c) with ΔTEC replacing ΔfoF2.

to 59° CGL under severely disturbed conditions represented by Q = 8. The auroral oval under steady magnetic conditions reaches its most equatorward extent near midnight and a consideration of the oval morphology as a function of the Q-index shows that Goose Bay could remain either an auroral or a subauroral station almost through the entire local night depending on the level of magnetic disturbance. Under conditions of moderate magnetic activity (Q ~ 3),however, Goose Bay remains an auroral zone station for about four hours around local midnight and it should be considered an ionospheric trough station during the remaining night hours.

Figure 2.2 shows the equatorward boundary of auroral optical emissions determined in the 2200 - 0200 LT sector by means of three widely different techniques as functions of Kp. The open circles represent $\Delta\lambda$, the separation between Goose Bay and the equatorward edge of continuous aurora as registered on the DMSP images and scaled by overlaying the 100-km grid on the images. Identification of the auroral boundaries and the actual scalings were performed on the original DMSP images archived at AFGL. Note that Figure 2.2 represents 48 individual DMSP images that afforded unambiguous determinations of the low latitude boundary of continuous aurora. A positive value of $\Delta\lambda$ signifies that the auroral boundary is located poleward of the Goose Bay station. The solid circles show the latitudinal separation of Goose Bay from the equatorward edge of the diffuse aurora, recognized as such on the basis of observations made from the ISIS-2 satellite (Anger and Lui, 1973; Lui and Anger, 1973; Lui et al., 1973; Lui et al., 1975a and Lui et al., 1975b). The 58 solid circles shown in the figure are adopted from the work of Lui et al., (1975a). The

dash-dot line is the low latitude boundary of the Feldstein auroral oval (Feldstein and Starkov, 1967). The dotted line and the continuous line represent linear regressions on the DMSP and ISIS-2 data respectively, the corresponding correlation coefficients being -0.770 and -0.715. Note that all three boundaries are determined near local midnight. The error bars show the sample standard deviation given in standard notation (Bendat and Piersol, 1971) as

$$S_{yx} = \left\{ \frac{1}{N-2} \left(\sum_{l=1}^{N} (y_l - \bar{y})^2 - \frac{\left[\sum_{l=1}^{N} (x_l - \bar{x})(y_l - \bar{y}) \right]^2}{\sum_{l=1}^{N} (x_l - \bar{x})^2} \right) \right\}^{\frac{1}{2}}$$

The regression equations are:

$$\Delta\lambda = -1.57Kp + 4.7 \qquad \left[\text{DMSP}\right],$$

$$\Delta\lambda = -0.99Kp + 2.7 \qquad \left[\text{ISIS-2}\right].$$

Figure 2.2 shows that the discrepancy between the equatorward boundaries of auroral luminosity monitored by the DMSP and ISIS-2 satellites is insignificant. The low latitude boundary of the Feldstein auroral oval, however, is located at lower latitudes in comparison to the satellite-based measurements. This result is in general conformity with previous observations made by Feldstein et al., (1969) who suggest that the cause of this solar cycle-associated variation could be changes occurring in the intensity of the ring current with the polar electrojets remaining unchanged.

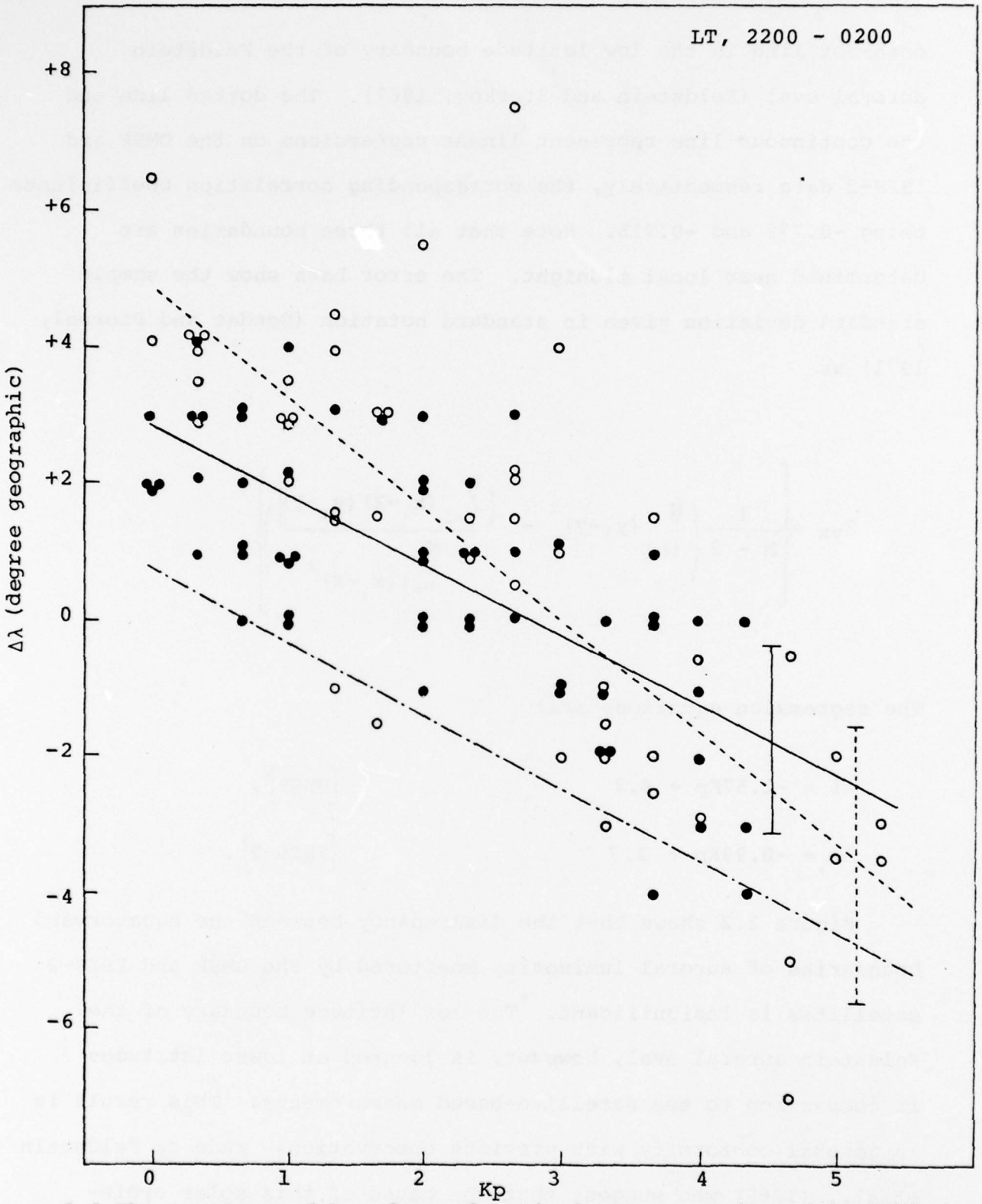

Figure 2.2 The equatorward boundary of optical aurora monitored by DMSP (open circles, dotted line) and ISIS-2(solid circles, solid line) measured as latitudinal separation from Goose Bay. The error bars represent the sample standard deviation. The dash-dot line shows low latitude boundary of Feldstein auroral oval.

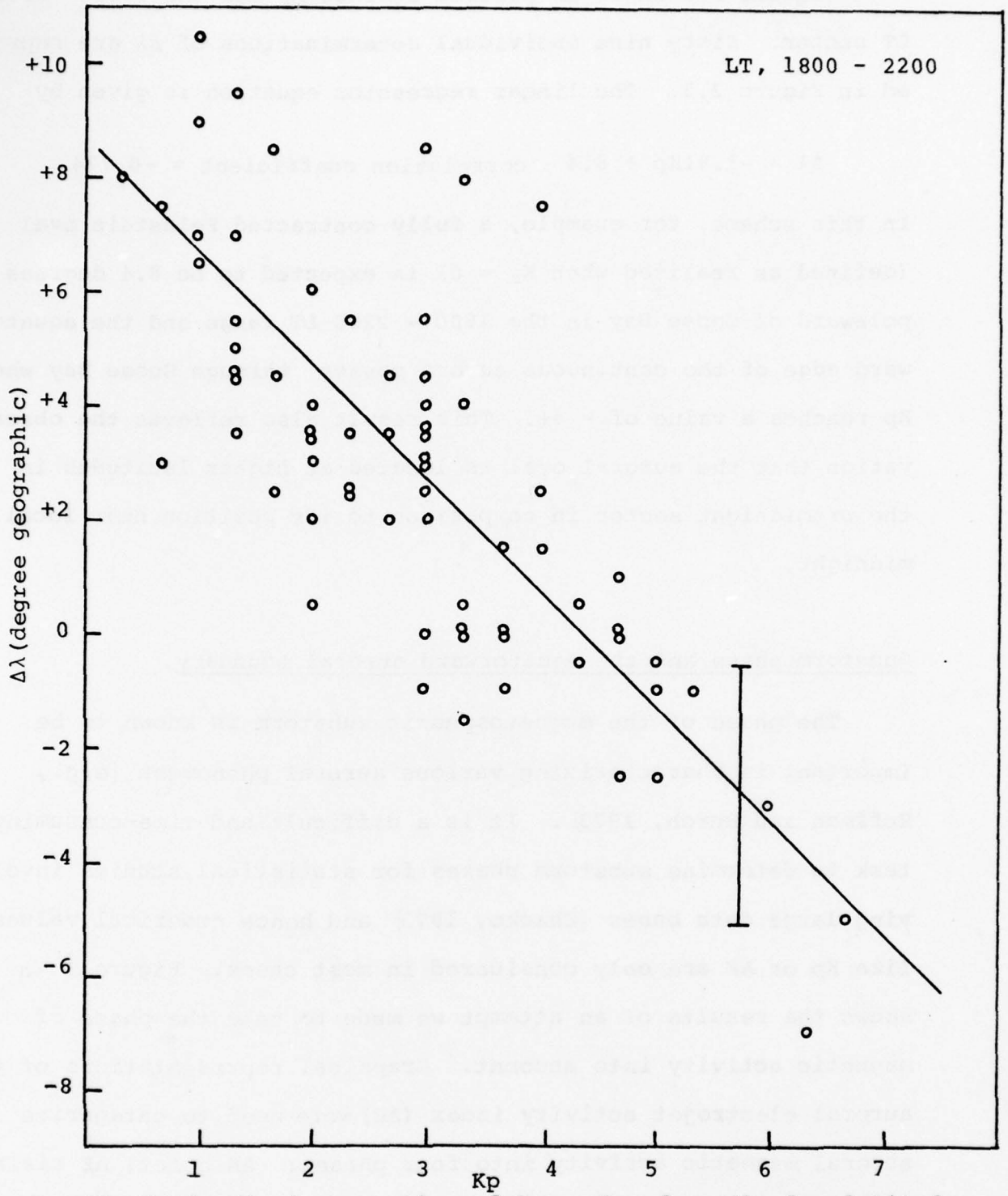

Figure 2.3 The latitudinal separation of Goose Bay from the low latitude edge of continuous aurora in the 1800-2200 LT sector vs Kp. The linear regression line and the sample standard deviation are shown.

Figure 2.3 shows $\Delta\lambda$ plotted against Kp for the 1800 - 2200 LT sector. Sixty nine individual determinations of $\Delta\lambda$ are represented in Figure 2.3. The linear regression equation is given by

$$\Delta\lambda = -1.91Kp + 8.4 \text{ ; correlation coefficient} = -0.774.$$

In this scheme, for example, a fully contracted Feldstein oval (defined as realized when Kp = 0) is expected to be 8.4 degrees poleward of Goose Bay in the 1800 - 2200 LT range and the equatorward edge of the continuous aurora passes through Goose Bay when Kp reaches a value of ~ 4+. This result also reflects the observation that the auroral oval is located at higher latitudes in the premidnight sector in comparison to its position near local midnight.

Substorm phase and the equatorward auroral boundary.

The phase of the magnetospheric substorm is known to be important in characterizing various auroral phenomena [e.g., Hoffman and Burch, 1973]. It is a difficult and time-consuming task to determine substorm phases for statistical studies involving large data bases [Chacko, 1975] and hence numerical values like Kp or AE are only considered in most cases. Figure 2.4a shows the results of an attempt we made to take the phase of magnetic activity into account. Graphical representations of the auroral electrojet activity index (AE) were used to categorize auroral magnetic activity into four phases: AE quiet, AE rising, AE maximum and AE falling. Clearly, this approach does not yield substorm phases but, as can be seen from the results, is adequate to organize auroral data in such a way as to take some cognizance of overall magnetic activity phase.

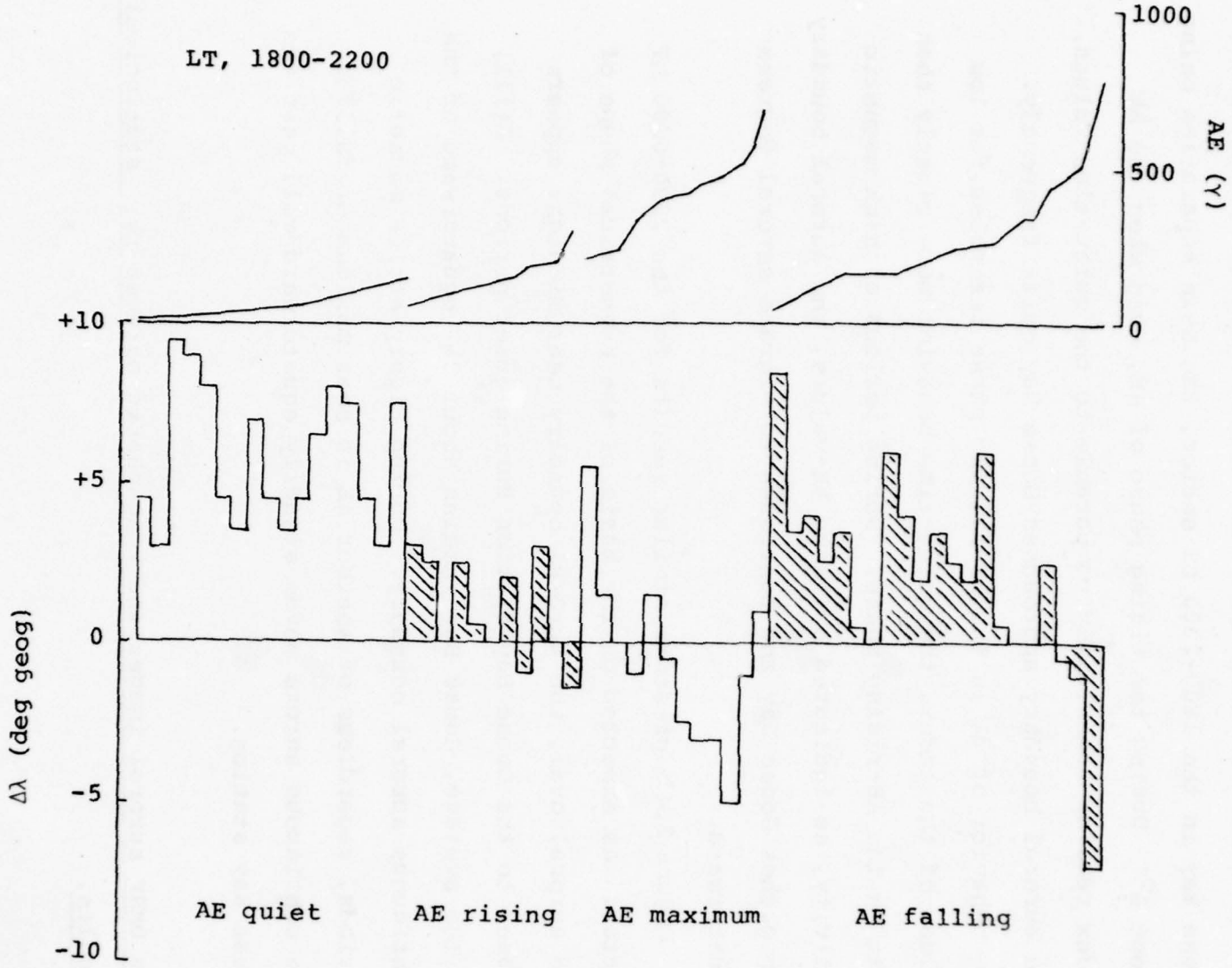

Figure 2.4 a The response of the low latitude boundary of the continuous aurora to changing AE index during different phases of auroral electrojet activity in the 1800- 2200 LT sector.

As AE remains quiet the equatorward boundary of the continuous aurora invariably remains several degrees poleward of Goose Bay in the 1800-2200 LT sector, the mean separation being about 5^{o}. During the rising phase of AE, even when the AE index remains numerically comparable to the quiet-time values, the auroral boundary approaches Goose Bay quite frequently. The behavior of $\Delta\lambda$ in the AE-falling phase resembles, for low values of the index, the quiet-time behavior more closely than that in the AE-rising phase. During periods of high magnetic activity, as indicated by large AE-values, the auroral boundary approaches Goose Bay and continues to migrate several degrees equatorward.

Figure 2.4b presents similar results for the 2200-0200 LT sector. As expected on the basis of the asymetrical shape of the auroral oval, the auroral boundary near midnight appears closer to the Goose Bay station during quiet periods. Still, on the average, Goose Bay remains about $2\frac{1}{2}^{o}$ equatorward of the continuous auroral boundary. During highly active magnetic periods, regardless of whether AE is near maximum or falling, the continuous aurora moves steadily equatorward well past the Goose Bay station.

<u>The DMSP auroral images and ionospheric parameters: statistical results</u>.

With increasing auroral activity the bottomside ionograms rapidly gain complexity and finally conditions that render them virtually unscalable set in. This circumstance severely limited

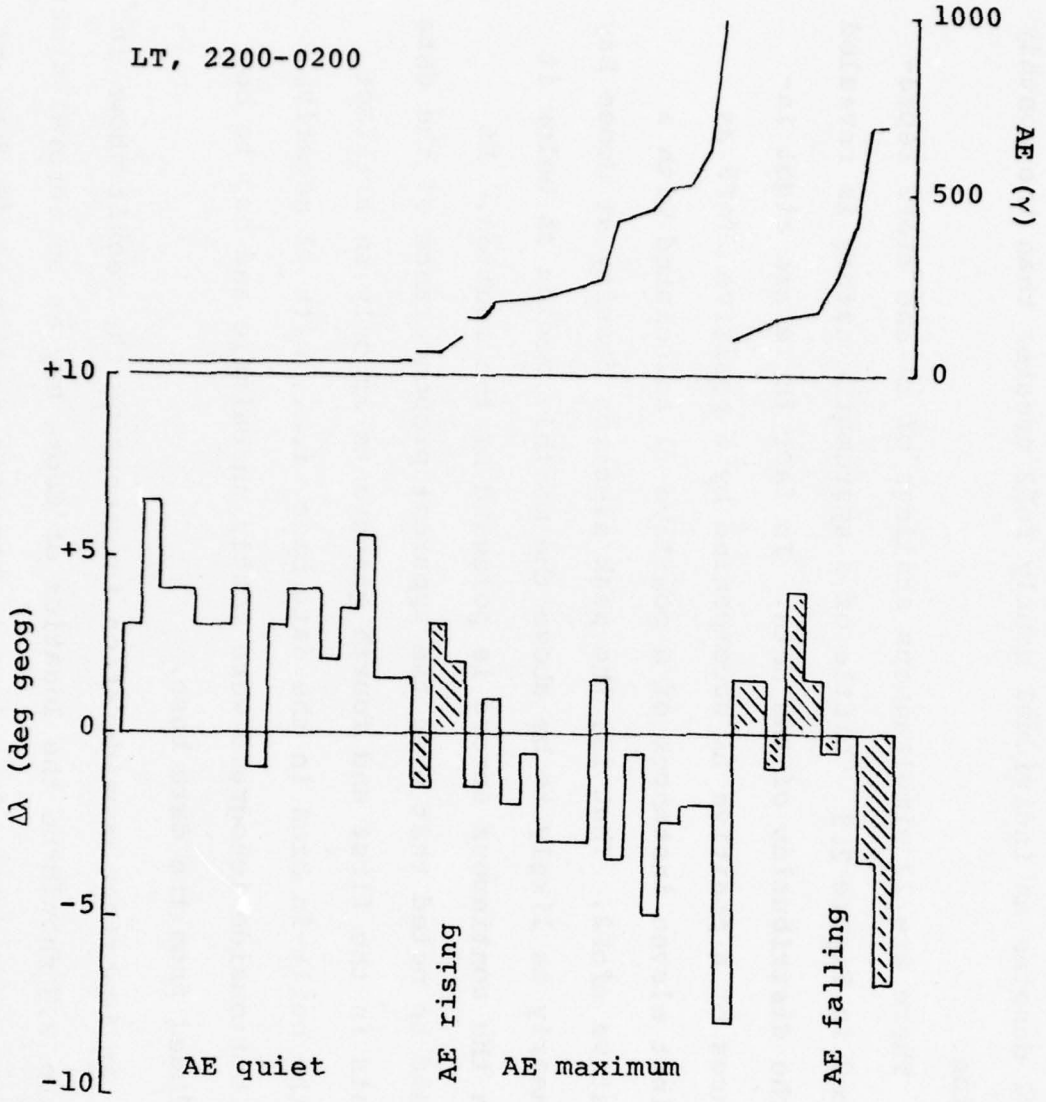

Figure 2.4b The response of the low latitude boundary of the continuous aurora to changing AE index during different phases of auroral electrojet activity in the 2200-0200 LT sector

the number of DMSP images with more or less simultaneously determined ionospheric parameters available for the present study, the net effect being a large attrition in data as seen in Figure 2.1. Figure 2.5 shows a plot of $\Delta\lambda$ against ΔfoF2 at Goose Bay, the latter quantity representing the deviation of the hourly foF2 value from the monthly median. Note that a positive value of ΔfoF2 denotes an individual hourly foF2 greater than the monthly median.

There are 27 simultaneous scalings of $\Delta\lambda$ and ΔfoF2 represented in Figure 2.5 Little of a systematic nature is revealed by the distribution of the data. In fact there are eight instances of a positive $\Delta\lambda$ accompanied by a positive ΔfoF2 as against eleven instances of a positive $\Delta\lambda$ associated with a negative ΔfoF2. That is, the peak electron density at Goose Bay is nearly as likely to be above the monthly median as below it when the continuous aurora is poleward of the station. It should be noted that even the apparent preponderance of the data points in the first and fourth quandrants is only an artifact of the built-in bias in the data base, i.e., with $\Delta\lambda$ negative, the bottomside ionograms were mostly unscalable and had to be excluded from the data base.

An important consideration in assessing the result shown in figure 2.5 should be the location of Goose Bay as an auroral station or a trough station depending on magnetic conditions (Buchau, et al., 1978) . However, the occurrence probabilities of the main trough quoted in the literature vary widely due to differences in the altitude of the observations, the experimental data resolution obtained and

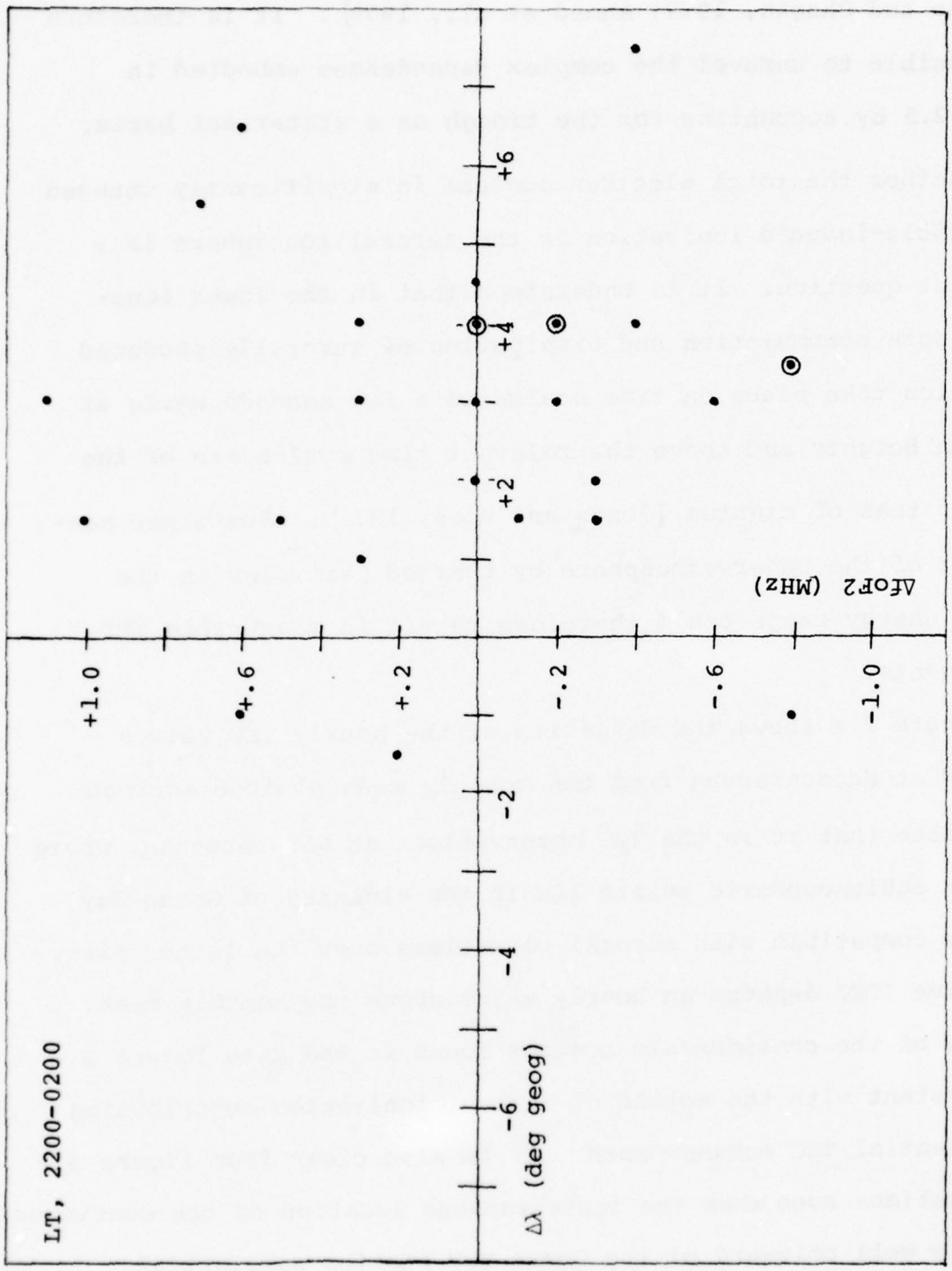

Figure 2.5 The separation of Goose Bay from the equatorward edge of the continuous aurora ($\Delta\lambda$) and the deviation of the hourly foF2 value from the monthly median (ΔfoF2) show no systematic relationship to each other.

the criteria used for defining the trough (Tulunay and Sayers, 1971; Brace and Theis, 1974; Feinblum and Horan, 1973; Halcrow, 1976; Mendillo and Chacko, 1977; Ahmed et al., 1979). It is therefore not possible to unravel the complex dependences embodied in figure 2.5 by accounting for the trough on a statstical basis.

Whether the total electron content is significantly changed by particle-induced ionization in the auroral ionosphere is a pertinent question. It is understood that in the lower ionosphere both accumulation and dissipation of aurorally produced ionization take place on time scales of a few seconds while at F-region heights and above the relevant time scales are of the order of tens of minutes [Jones and Rees, 1973]. Sustained bombardment of the upper atmosphere by charged particles in the auroral energy range could therefore result in measurable TEC enhancements.

Figure 2.6 shows the deviation of the hourly TEC values measured at Narssarssuaq from the monthly mean plotted against $\Delta\lambda$. Note that it is the TEC observations at Narssarssuaq, whose F-region subionospheric points lie in the vicinity of Goose Bay, that are compatible with auroral conditions over the latter site. A positive ΔTEC denotes an hourly value above the monthly mean. In spite of the considerable scatter found in the data, figure 2.6 is consistent with the notion of auroral ionization contributing to substantial TEC enhancements. It is also clear from figure 2.6 that sometimes even when the instantaneous location of the continuous aurora is well poleward of the Goose Bay station substantial enhancements of TEC may occur.

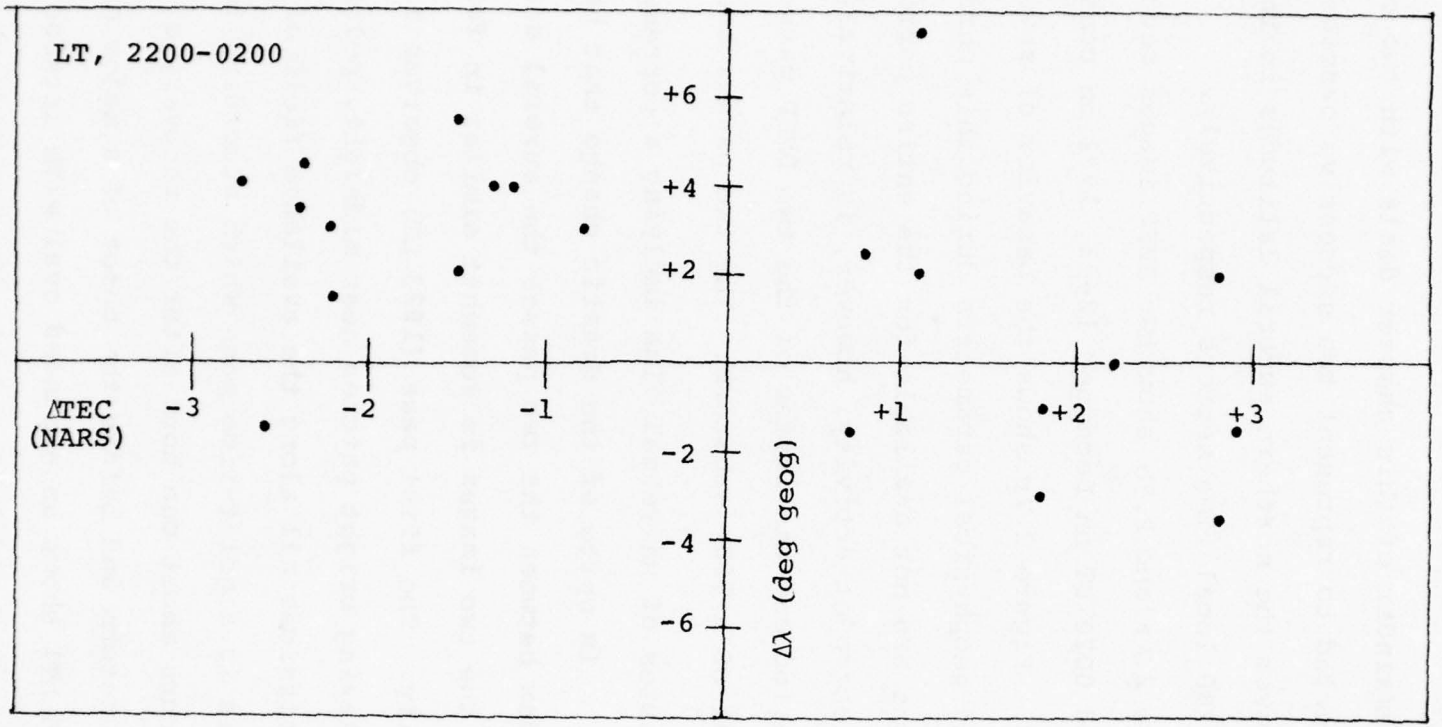

Figure 2.6 The distribution of $\Delta\lambda$ against ΔTEC(Narssarssuaq) is largely consistent with the notion of auroral ionization contributing to substantial TEC enhancements.

DMSP auroral images and ionospheric parameters: two case studies. December 12-13, 1972

The remainder of this chapter deals with two case study events selected to represent two successive passages of the DMSP satellite over the northern auroral latitudes in the 1800-2200 and 2200-0200 local time sectors respectively.

Figure 2.7 a and 2.7b show two DMSP images recorded at 2238 UT and 0020 UT on December 12-13, 1972 on consecutive traversals. Figure 2.7c shows the behavior of several ionospheric and geophysical parameters during this period. IMF observations are not available for the entire period. The auroral electrojet activity, however, is relatively unambiguous in this period and the latter of the two DMSP passes takes place at the peak of a 700γ substorm. The two passes are separated by 102 minutes of universal time implying a corresponding LT change at Goose Bay. In spite of the drastic change that has occured in the AE index between the two passes the auroral activity represented by the two images is somewhat similar in form though not in intensity. The first pass (1823 LT) observes a contracted oval displaying bright patches near midnight, polar cap arcs and diffuse emissions all along the available field of view of the oval. This is a quiet-time pass which according to the AE index, occurs about one hour after the recovery of a moderate (~250γ) substorm and before the onset of a major one. The next pass (2005 LT) shows an expanded oval with intense auroral emissions around midnight and, in the pre-midnight sector, quiet arcs that form the poleward border of the diffuse aurora.

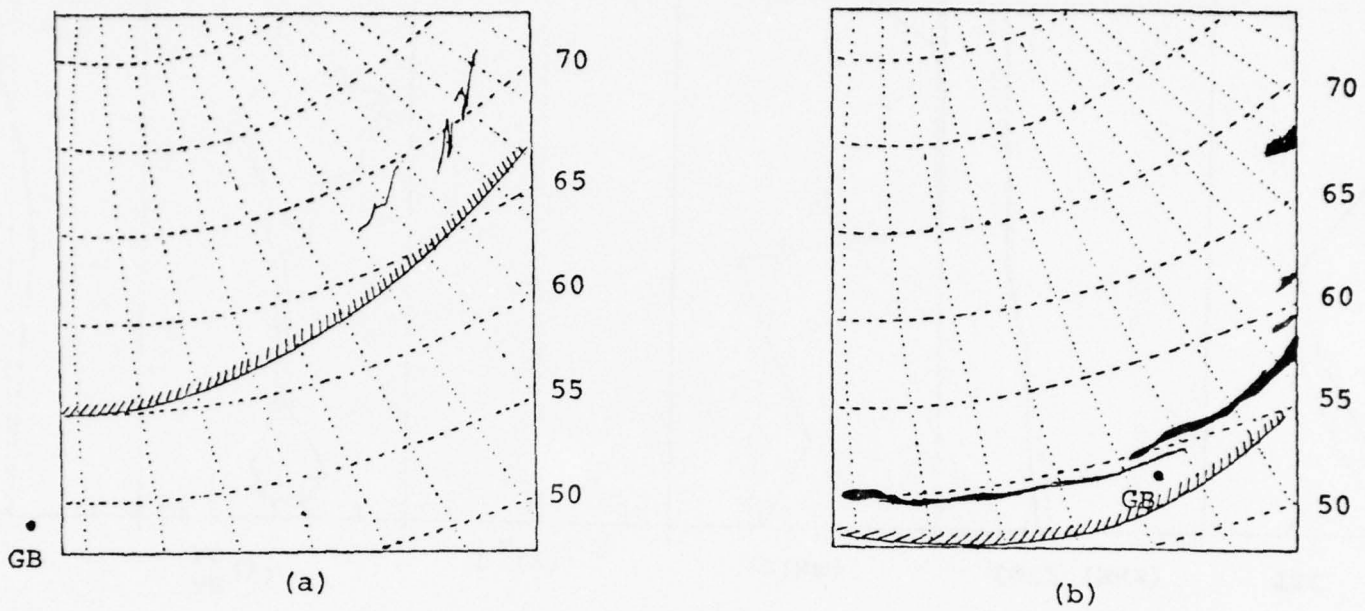

Figure 2.7 Two DMSP images recorded at 2238 and 0020 UT on December 12 - 13, 1972. The location of Goose Bay is marked. The equatorward boundary of the continuous aurora and, in (b) the location of the discrete arcs are shown. Local times at Goose Bay are 1823 and 2005, respectively.

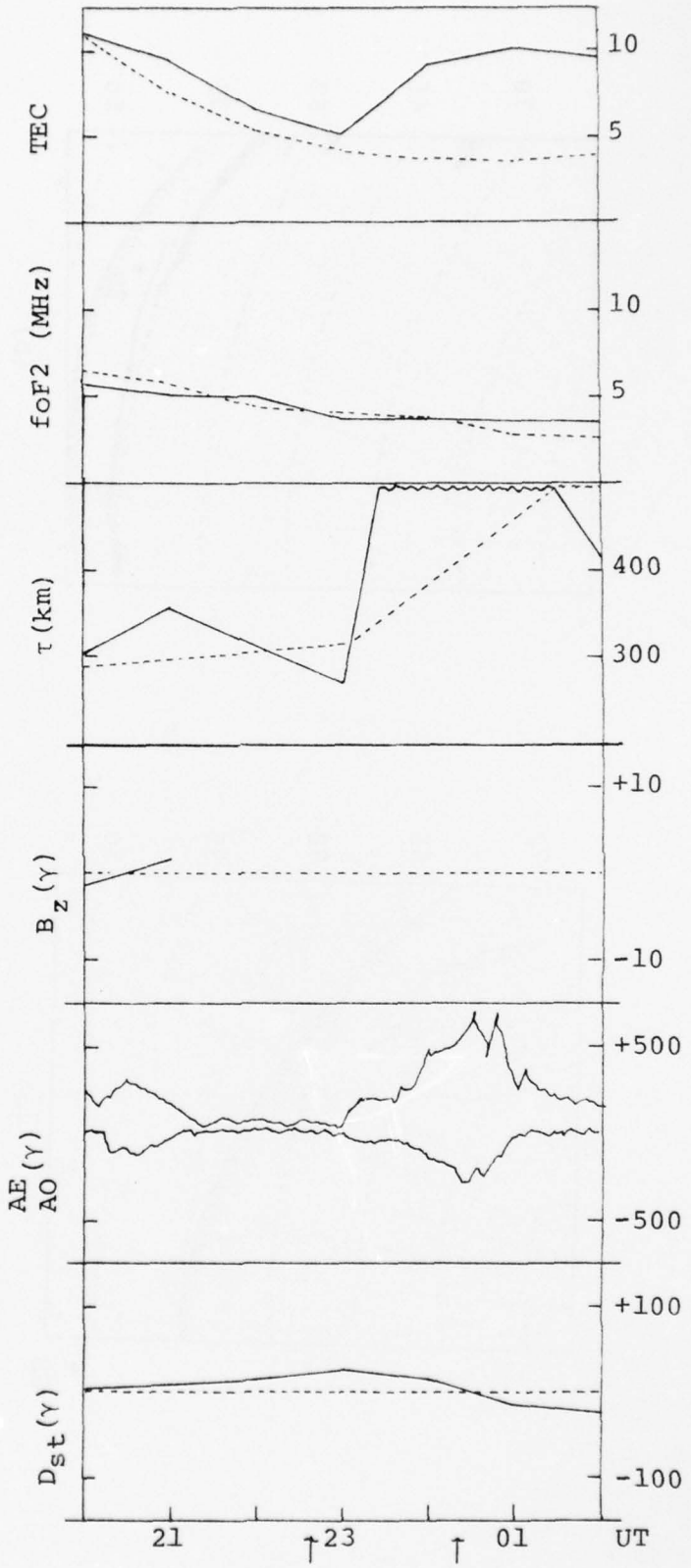

Figure 2.7c Ionospheric and geophysical parameters during the UT interval 2000 - 0200 on December 12 - 13, 1972

The ionospheric parameters presented in Figure 2.7c are TEC (Narssarssuaq), foF2 (Goose Bay) and the slab thickness τ. All through the 2000-0200UT period, foF2 remains close to the monthly mean revealing little more than the steady depletion suffered by the ionosphere on the night side. The total electron content and slab thickness, on the other hand, register dramatic enhancements between the two passes in conjunction with rising auroral electrojet activity. $\Delta\lambda$ values also show one of the most abrupt changes observed in this study, namely from $+7\frac{1}{2}^{o}$ to -1^{o}. It is clear in this instance that rapid equatorward expansion of the auroral precipitation region past the Goose Bay latitude has resulted in a very large enhancement in the total ionization without a corresponding increase in foF2. (See the Discussion section for previous related work).

November 5, 1972

The two DMSP images represented in Figures 2.8a and 2.8b show the midnight to early morning sector of the auroral domain. Figure 2.8a depicts a classic example of the continuous aurora that remains uniform in intensity all along the visible segment of the auroral region in a band aligned with the magnetic latitude. Poleward of the diffuse emissions are found several quiet, discrete arcs all of which also appear to be magnetic-latitude-aligned. This quiet but well-defined auroral activity is confined to a relatively contracted oval. Goose Bay is located $\sim 3\frac{1}{2}^{o}$ equatorward of the boundary of the continuous aurora and the nearest discrete arc appears $\sim 5\frac{1}{2}^{o}$ poleward. The general level of auroral activity found in the subsequent

pass (Figure 2.8b) is the same as that seen 102 minutes earlier in the previous pass. The diffuse emissions have suffered some apparent loss of intensity and the polewardmost discrete arcs are more active. The oval appears to have undergone no significant expansion or contraction and in fact the magnetic-latitude-aligned character of both continuous and discrete auroral displays is preserved. Goose Bay, however is now further removed from the diffuse aurora owing to the poleward migration of the auroral oval with local time that occurs in this sector. Figure 2.8c shows several geophysical and ionospheric parameters between 0300 and 0900 UT on November 5, 1972 in the same format as that of Figure 2.7c . All geophysical indications are consistent with the characterization of both these passes as quiet-time, contracted oval traversals of the auroral latitudes: AE is very low and constant and the IMF is northward and more or less steady.

The TEC values are remarkably constant and deviates little from the monthly mean. The critical frequency foF2, on the other hand, shows large deviations from the monthly mean all through the local early morning hours. The slab thickness shows corresponding deviations. The large, negative foF2 values are consistent with the location of the continuous aurora well poleward of the Goose Bay latitude.

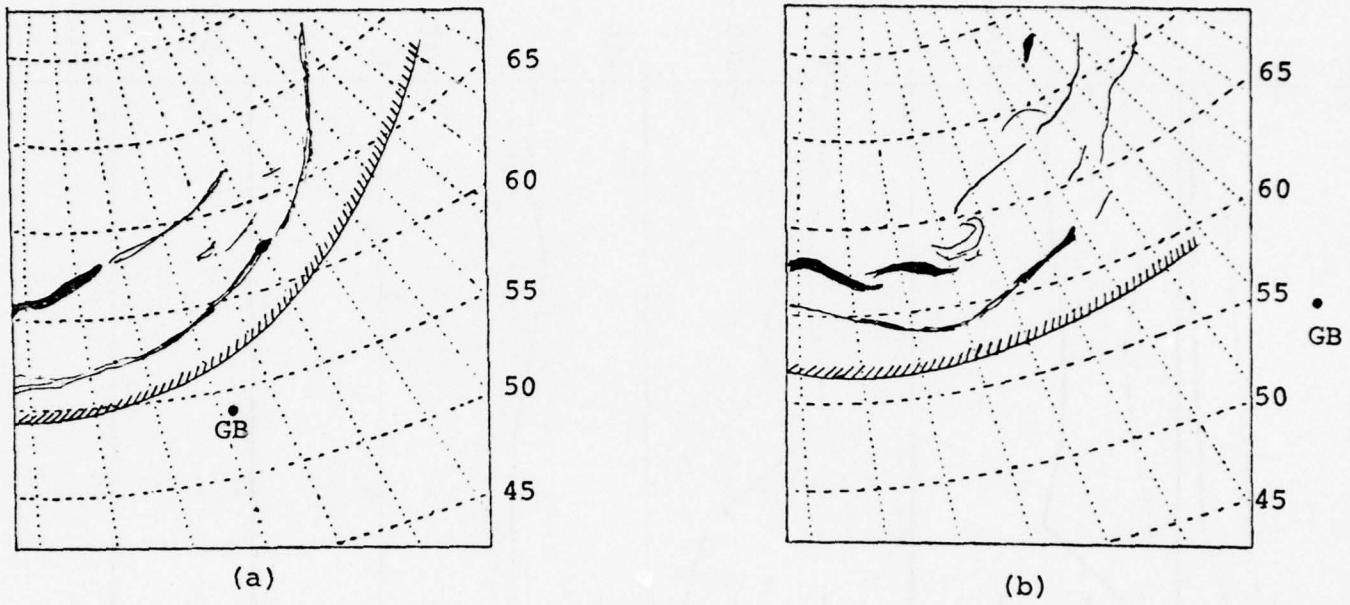

Figure 2.8 Two DMSP images recorded at 0524 and 0706 UT November 5, 1972. The location of Goose Bay is marked. The positions of the equatorward boundary of the continuous aurora and discrete aurora are shown. Local times are 0109 and 0251, respectively.

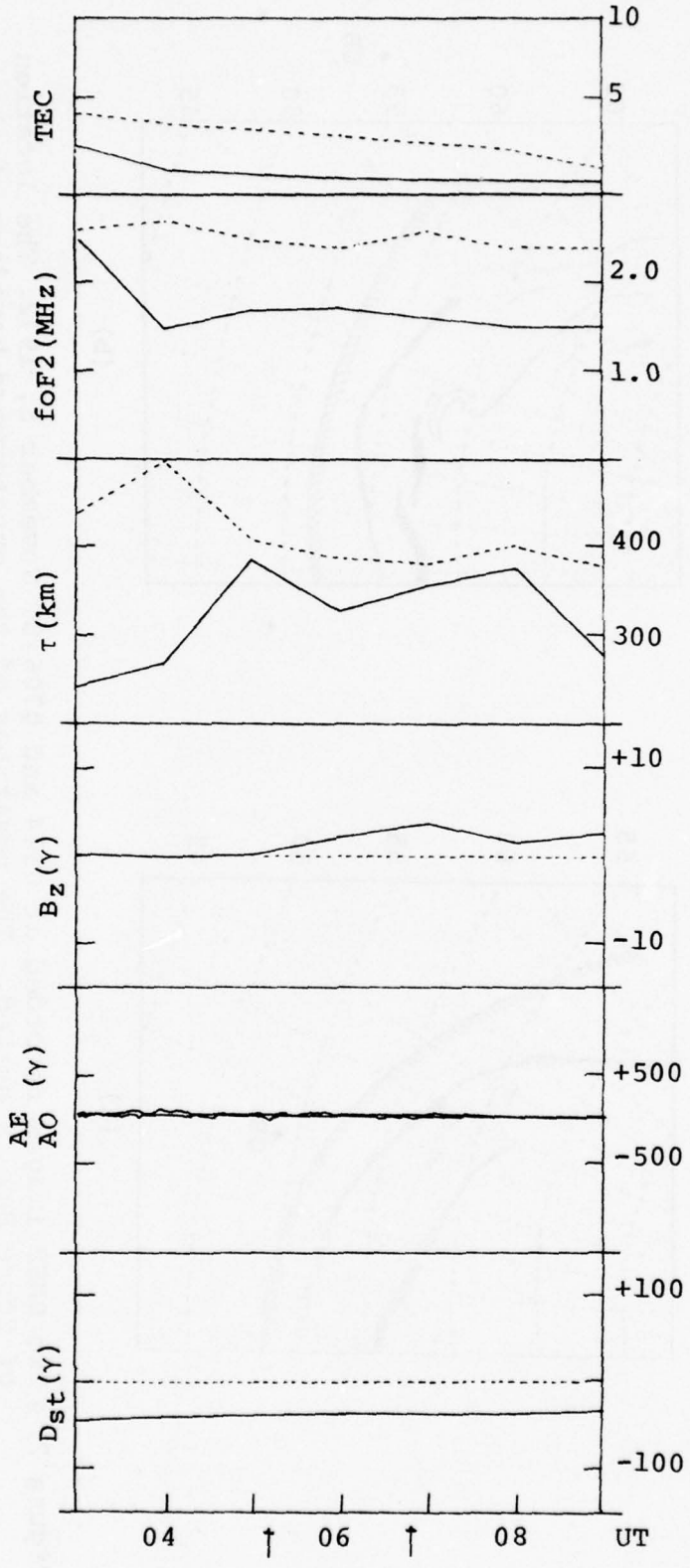

Figure 2.8c Ionospheric and geophysical parameters during the UT interval 0300 - 0900 on November 5, 1972.

CHAPTER 3. DISCUSSION AND CONCLUSIONS

The principal outcomes of this study may be summarised as follows.

1. The low latitude boundaries of auroral luminosity detected by the DMSP and ISIS satellites are very nearly coincident on a statistical basis. However, this common boundary lies poleward of the low latitude edge of the Feldstein auroral oval, possibly signifying a solar cycle-related variation

2. The proximity of the equatorward edge of the continuous aurora to the Goose Bay station (i.e., the size of the auroral oval) depends not only on the magnitude of the AE index but on the phase of the AE activity. For example, in the 1800 - 2200 LT sector, during the rising phase of auroral electrojet activity, the auroral boundary appears closer to Goose Bay even when the AE index remains numerically comparable to the quiet-time values.

3. Past studies using topside sounder data showed, on a statistical basis as well as in individual instances, that the electron density enhancements in the F-region associated with the poleward wall of the main electron density trough occur a few degrees equatorward of the low latitude boundary of optical auroral emissions as determined by ISIS and DMSP auroral images. Very little of a systematic nature could be deduced from the present

effort which examined the relationships between the presence of auroral activity near Goose Bay as revealed on DMSP images and the ionospheric parameters ΔfoF2 and ΔTEC.

The low latitude boundary of optical aurora monitored by DMSP, ISIS and all-sky camera.

The diffuse aurora monitored by the ISIS-2 satellite is considered to be generated mainly by relatively softer electrons arriving from the inner edge of the plasma sheet (Lui et al., 1977). Mizera et al., (1975) have concluded that the more energetic component of the precipitating electron spectrum is responsible for the major part of the optical intensity received by the DMSP detector. Meng et al., (1979) does not make the distinction between the diffuse aurora and the continuous aurora and state, on the basis of comparisons between precipitating electrons responsible for the diffuse emissions in the evening sector and their parent populations in the magnetospheric equatorial plane, that the plasma sheet proper is the source region for diffuse auroral precipitations.

The DMSP satellites register spectral emissions in the 6,000 to 10,000Å (full-width at half maximum) range using a line scanning radiometer (Pike, 1975). The scanning auroral photometer on board ISIS-2 detects a few prominent auroral spectral lines individually (Lui and Anger, 1973; Shepherd et al., 1976), thereby affording not only the best-defined quantitative observation of auroral intensity but estimates of the energy spectrum of the precipitating particles as well. Pike and Whalen (1974) argue, on the basis of the relative contributions made by the dominant auroral spectral lines to the all-sky camera range and the DMSP detector range, that approximate proportionality should exist between the two and hence the spatial

patterns of the auroras observed by the two techniques should be the same. Eather (1978) has reviewed the development and characteristics of the DMSP detectors and found their sensitivity on a par with or better than that of all-sky cameras.

Viewed against this background the interrelationships depicted in Figure 2.2 may be understood in the following terms. 1). On a statistical basis there is little to recommend drawing a distinction between the diffuse aurora (ISIS) and the continuous aurora (DMSP). 2). The DMSP observations are characterized by larger scatter and at very low Kp levels (≤ 1) the ISIS-2 observations tend to delineate a lower latitude auroral boundary. In the absence of intercalibraions between the ISIS and DMSP detectors it is not fruitful to try to choose among the various scenarios, based on relative sensitivities of these two instruments, that could lead to the above results. If it is assumed that the ISIS-2 measurements represent a better evaluation of auroral luminosity, on the basis that the experiment is well-defined and designed specifically for monitoring auroral emissions, the extra scatter in the DMSP data may possibly be attributed to variations in the gain levels of the radiometer dictated not necessarily by auroral exigencies. 3). The mean position of the Feldstein auroral oval low latitude boundary lies significantly equatorward of the mean positions of the two satellite-defined auroral low latitude boundaries. The Feldstein and ISIS-2 boundaries maintain a nearly constant 2°-separation along the entire Kp range considered. In view of Eather's (1978) finding that the DMSP detectors possess sensitivities at least as good as those of all-sky cameras the explanation that suggests itself is an intriguing one. The Feldstein and Starkov (1967) observations upon which the dash-dot line of Figure 2.2

is based were made during 1957 - 1959 when the yearly mean Zurich sunspot numbers were 190.2, 184.8 and 159.0 respectively. Both sets of satellite observations were made in the 1971 - 1973 period when the yearly mean Zurich sunspot number values were 69.7, 66.8 and 39.3. Feldstein et al., (1969) suggest the possibility of a solar cycle-associated variation in the auroral oval boundaries caused by changes occurring in the intensity of the ring current with the polar electrojets remaining unchanged.

Substorm phase and auroral boundaries.

The role of substorm phase in auroral dynamics has been recognized before (Akasofu, 1968, Eather and Mende, 1973; Hoffman and Burch, 1973). On account of the sheer volume of labor involved in the effort to identify individual substorms and the attendant uncertainties, few workers have explicitly considered the substorm phase in statistical studies involving large data bases. We sought to incorporate the phases of the auroral electrojet activity into the present study as a crude measure of the phases of substorms themselves although the limitations of the AE index as an indicator of substorms are well-recognized (e.g., Kamide and Winningham, 1977). The results of this effort presented in Chapter 2 establish that for the same general level of magnetic activity indicated by the magnitude of the AE index, the response of the auroral boundary is vastly different during AE-rising and AE-falling phases.

The information given in Figures 2.4a and 2.4b may be utilized to derive numerical estimates of the proximity of the auroral boundary to a midnight station as a function of the AE index magnitude and phase.

The optical aurora and auroral ionization.

The bulk of the ionization produced by precipitating auroral particles on the night side occurs between 100 and 150 km along field lines containing the precipitation (Rees, 1963). At these heights the characteristic times for build-up and decay of ionization are a few seconds (Jones and Rees, 1973) i.e., ionization enhancements are more or less simultaneous with particle precipitations and auroral emissions at low altitudes. If however, the build-up and dissipation of ionization at F-region heights are considered, the characteristic time-scales turn out to be tens of minutes (Jones and Rees, 1973; Knudsen, 1974; Whitteker, 1977). This could happen as a result of in-situ production by very soft particles, atmospheric heating by precipitating energetic particles and consequent upwelling of plasma or by plasma diffusion.

The time lag of tens of minutes between particle precipitation (∿optical emissions) and the emergence of its ionization signature in the upper ionosphere is crucial to the explanation of the observed equatorward displacement of the latter with respect to the former (Chacko and Mendillo, 1977). We believe plasma is being transported equatorward from the production region within this time interval. Collisional coupling with an equatorward neutral wind generated by auroral heating could move auroral ionozation to lower latitudes and upwards (Bates et al., 1973). A more likely cause would be $\underline{E} \times \underline{B}$ drifts coupled with upward diffusion.

The dawn-to dusk magnetospheric electric field, when mapped down the field lines to polar regions by assuming the lines to be equipotentials, produces ionospheric convection shown schematically in Figure 3.1. The position of Goose Bay at midnight corresponds to the 'T' in the label TROUGH in the figure. Considering representative values, a drift velocity component of 0.2 km/sec operating for 30 minutes will result in a 3.6° displacement, well in accord with the findings reported by Wagner et al., (1973) and Chacko and Mendillo (1977). Thus the evolution of F-region ionization is determined not only by chemistry and upward diffusion but by equatorward transport as well.

The paucity of E-region data compatible with the rest of the observations discussed in this report precluded the incorporation of E-region information into our considerations on a statistical basis. It may be noted, however, that the Chatanika incoherent scatter radar observations (Vondrak and Barron, 1976) show that the bulk of the ionization accompanying visual aurora is well confined to E-region altitudes, with much smaller enhancements simultaneously observed above a height of ~200 km.

Narssarssuaq TEC enhancements incorporate an E-region component along the slanted ray path. We have used hourly values of TEC in this study, thereby suppressing the great variability and fine structure associated with the E-region contribution to TEC enhancements at auroral latitudes.

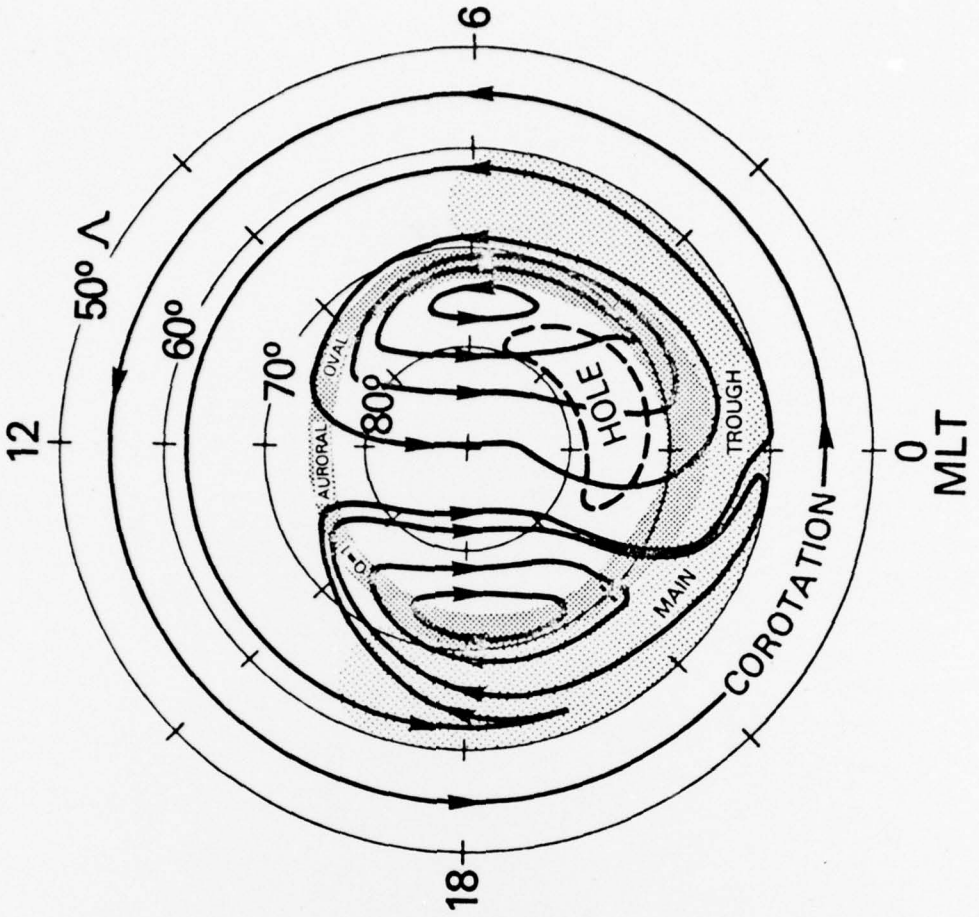

Figure 3.1 Typical plasma drift configuration across the polar cap superimposed on several high latitude ionospheric and auroral phenomena (after Brinton et al., 1978)

Appendix

VOL. 83, NO. A12 JOURNAL OF GEOPHYSICAL RESEARCH DECEMBER 1, 1978

The High-Latitude Behavior of hmF_2 and NmF_2 Along the Noon-Midnight Meridian Under Quiet Conditions

C. C. CHACKO

Department of Astronomy, Boston University, Boston, Massachusetts 02215

The mean latitudinal (corrected geomagnetic) variation of the F_2 peak parameters hmF_2 and NmF_2 from mid-latitudes to high latitudes along the noon-midnight meridian is established for midwinter quiet time conditions using Isis 2 topside sounder data.

The chief purpose of this brief report is to furnish ionospheric workers with some handy information on the average behavior of the F_2 peak from mid-latitudes to high latitudes under what may be deemed an optimum set of geophysical conditions. The variation of hmF_2 and NmF_2 has been extensively monitored at individual sites using bottomside sounders [e.g., *Thomas et al.*, 1957; *Becker*, 1967]. Although such observations made along a closely spaced meridian chain of stations might reveal the latitude dependence of hmF_2 and NmF_2, the requisite data do not seem to exist at present. On account of the large number of variables on which hmF_2 and NmF_2 are known to depend (solar zenith angle, local time, season, solar cycle, neutral winds, magnetic activity, heating, E fields, and auroral particle fluxes), available topside sounder data are usually too meager to afford a consistently constructed mean representation of the latitude dependence of the F_2 peak parameters; observations spanning several months in different years under wide ranges of Kp values may have to be lumped together to arrive at large enough data bases that yield statistically satisfactory mean results.

In December 1971 the topside sounder on board the Isis 2 satellite, which maintained a polar orbit at a near constant altitude of ~1400 km close to the noon-midnight meridian ($\lesssim 1\frac{1}{2}$ hours LT), performed soundings of the northern hemispheric ionosphere at a rate rapid enough to furnish, on the average, about three good quality ionograms every 2° of latitude. A majority of these were obtained during periods characterized by Kp values of $\leq 1+$. What follows deals with the mean behavior of the F_2 peak parameters hmF_2 and NmF_2 from ~45° to 80° corrected geomagnetic latitude (CGL) determined by using topside soundings made near the noon-midnight meridian during a 21-day period about the winter solstice under very quiet magnetic conditions. The mean Zurich sunspot number for December 1971 was 69 [*National Climatic Center*, 1973]. The narrow ranges of the variables (local time, Kp, season, and solar cycle) associated with the data base assure the usefulness of the mean results presented here as basic representations for the latitude dependence of the appropriate parameters. Note that in general the derived values of hmF_2 are considered less reliable than the values of critical frequency scaled directly from topside or bottomside ionograms. Typically, hmF_2 values derived from topside ionograms are too large by ~10 km on account of the critical echoes emanating from regions above the F_2 peak rather than from the peak itself [*Jackson*, 1969]. Concerning the present data base, the nightside results should be statistically more reliable than the dayside results owing to the larger number of observations available on the nightside. Note also that this brief report is complementary to two recent studies that utilized parts of the same data base for detailed investigations of the main electron density trough on the nightside [*Mendillo and Chacko*, 1977] and the cusp-related electron density enhancements on the day side [*Chacko and Mendillo*, 1977].

Figure 1*a* shows average values of hmF_2 and NmF_2 from 40°N to 80°N CGL at half-degree intervals. The topside sounder data were obtained on 30 traversals of the northern hemisphere between December 7 and 28, 1971. The relevant segments of the satellite track lay within $1\frac{1}{2}$ hours of the midnight meridian during this period. Figure 1*a* has contributions from a total of 1233 ionograms recorded during quiet magnetic intervals ($Kp \leq 1+$). Not all the 30 passes yielded data in the entire 40°–80° CGL range; on the average, the mid-latitude (~55° CGL) values of hmF_2 and NmF_2 represent the mean of ~16 observations, while the high-latitude (~75° CGL) values represent the mean of ~20 observations. Data obtained from the poorest quality ionograms were excluded. The vertical bars represent standard deviations.

The latitude range on the nightside encompassed by Figure 1*a* is dominated by the main electron density trough [*Muldrew*, 1965; *Rycroft and Burnell*, 1970; *Tulunay and Sayers*, 1971; *Feinblum and Horan*, 1973; *Halcrow*, 1976; *Mendillo and Chacko*, 1977] and, poleward of the trough, by the auroral ionosphere. The latter region is marked by highly variable latitudinal distributions of electron densities [*Pike*, 1972; *Brinton et al.*, 1978]. The trough that appears in mean NmF_2 in Figure 1*a* is centered at ~59° CGL, nearly 9° wide (2 MHz) and has a poleward wall that is considerably steeper than the equatorward wall, the gradients being $\sim 14 \times 10^3$ el/cm³ deg and 6×10^3 el/cm³ deg, respectively.

The hmF_2 curve in Figure 1*a* reveals three latitudinal regions characterized by distinct mean hmF_2 behavior. The mean altitude of the F_2 peak remains nearly constant at 361 ± 10 km up to ~55° CGL. In this latitude range, NmF_2 monotonically decreases to its minimum mean value of $\sim 5 \times 10^4$ el/cm³. The latitudes including, and poleward of, the auroral ionosphere (~64°–80° CGL) are marked by a lower constant mean hmF_2 level of 312 ± 12 km. The transition from a 361-km mid-latitude mean hmF_2 to a 312-km high-latitude mean hmF_2 takes place over the CGL range of ~55°–64° occupied by the main electron density trough and yields a gradient of ~5.5 km/deg.

Figure 1*b* shows an individual Isis 2 pass (December 15, 0612 UT, 65°N CGL) during a quiet interval ($Kp = 1-$). Note that the large fluctuations in both NmF_2 and hmF_2 that the topside sounder detects, especially at the higher latitudes, have been smoothed out in the gross averages appearing in Figure 1*a*. The second region of depleted electron density found centered at ~72° CGL in Figure 1*b* represents a well-developed example of a feature frequently encountered in latitudinal

Copyright © 1978 by the American Geophysical Union.

Paper number 8A0711.

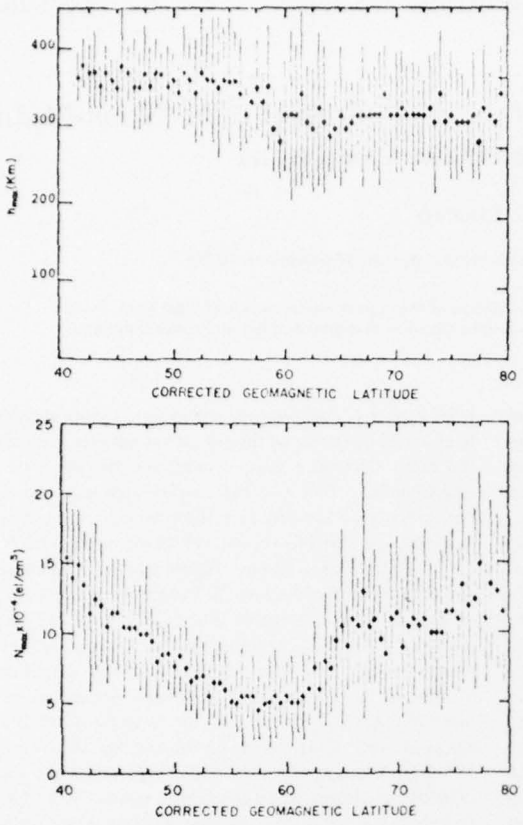

Fig. 1*a*. (Top) Mean h_{max} and (bottom) mean n_{max} near midnight meridian for midwinter quiet time conditions, constructed by using 30 Isis 2 orbits (topside sounder data) made between December 6 and 27, 1971; $Kp \leq 1+$.

electron density profiles [*Mendillo and Chacko*, 1977; *Brinton et al.*, 1978]. The mean behavior depicted in Figure 1*a* is not expected to represent adequately latitudinal features that are too narrow, too unstable in latitudinal position, or of too infrequent occurrence.

Figure 2*a* represents the counterpart of Figure 1*a* near local noon. There are considerably fewer soundings available on the dayside under geophysical conditions similar to the optimum ones specified for the local midnight observations. The average curves of hmF_2 and NmF_2 shown in Figure 2*a* are constituted by data from 453 ionograms. The number of soundings at mid-latitudes (~55° CGL) is about four, while that at high latitudes (~75° CGL) is about 14. Note that the ionograms obtained on the dayside, though fewer in number, are generally of better quality and lend themselves to more accurate scalings. The most prominent trend to be observed in the hmF_2 curve is its steady rise with increasing latitude in the 55°–70° CGL range. In the middle of this transition region (57°–67° CGL) the mean hmF_2 curve rises at a rate of ~5 km/deg. The NmF_2 curve shows that this latitude interval is marked by steadily decreasing densities which may be characterized by an average gradient of ~40 × 10^3 el/cm³ deg. Poleward of this region, in the 70°–80° CGL range, one expects the effects of precipitating magnetosheath particles to manifest themselves during quiet times [*Frank*, 1971; *Heikkila and Winningham*, 1971; *Burch*, 1972]. Prominent enhancements in plasma temperature and density in the topside ionosphere have been observed at these latitudes [*Titheridge*, 1976; *Chacko and Mendillo*, 1977]. Figure 2*a* locates the latitude of the cusp-related NmF_2 enhancement at 77.5° CGL and gives a peak-to-minimum ratio of ~2.3. The mean hmF_2 values in the 70°–80° CGL range exhibit large fluctuations. Nevertheless, it is convenient to assign a nominally constant value of ~297 ± 19 km to the mean height of the F_2 peak at these latitudes under the geophysical conditions specified previously. At mid-latitudes (<55° CGL), hmF_2 may possess a very weak magnetic latitude dependence, namely, a slight negative slope, but again one may assign a nominally constant value of ~254 ± 11 km to the mean height of the F_2 peak between 45° and 55° CGL for these conditions.

In midwinter, during periods of prolonged magnetic quiet, the latitudinal distribution of NmF_2 from mid-latitudes to high latitudes near local noon is known to follow the pattern seen in Figure 2*a* [*Chacko and Mendillo*, 1977]. Figure 2*b* shows the northern hemispheric dayside segment of an Isis 2 orbit at 0013 UT (65°N CGL) on December 9, 1971. This orbit which started towards the end of a *QQ* day represents a quiet time traversal, although *Kp* was raised from 1− to 2− on account of magnetic activity that commenced in the latter half of the first 3-hour period on December 9. Figure 2*b* shows the pattern of a quiet time midwinter pass near the noon meridian: with increasing latitude the peak electron density drops steadily until it is interrupted by a narrow column of enhanced ionization near 77° CGL. The interplanetary magnetic field remained steady (~6.2 γ) and northward for several hours prior to the pass [*King*, 1975], and the observed location of the *F* region signature of precipitating magnetosheath particles conforms to the known latitude of the dayside magnetospheric cusp under quiet conditions [*Burch*, 1972; *Yasuhara et al.*, 1973].

The data base utilized in this study is distinguished by remarkably narrow ranges of the relevant geophysical variables

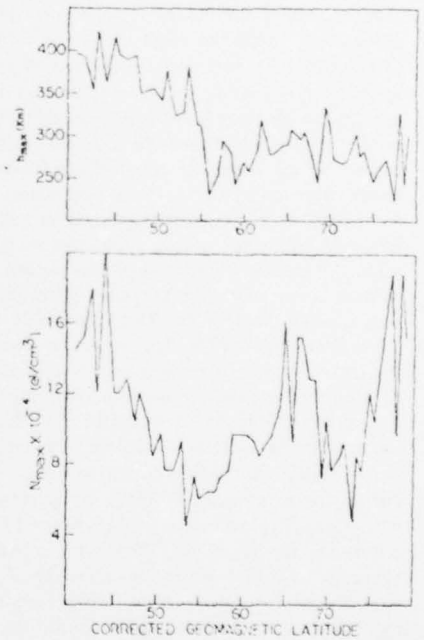

Fig. 1*b*. An individual quiet time Isis 2 pass near the midnight meridian. One of the 30 constituents of Figure 1*a*, this orbital segment was traversed between 0605 and 0618 UT on December 15, 1971; Kp = 1 −. Note the second, higher latitude ionization depletion centered at ~72° CGL [*Brinton et al.*, 1978].

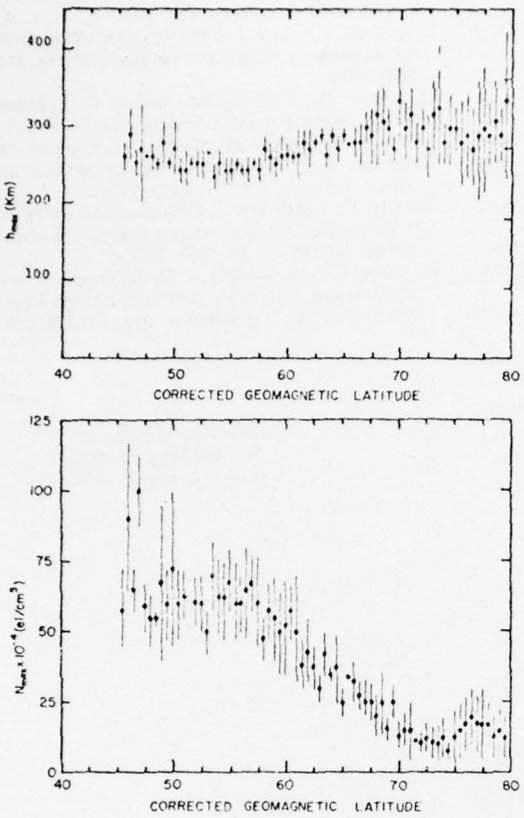

Fig. 2a. (Top) Mean h_{max} and (bottom) mean n_{max} near noon meridian for midwinter quiet time conditions, constructed from 15 Isis 2 orbits (topside sounder data) made between December 6 and 27, 1971; $Kp \leq 1+$.

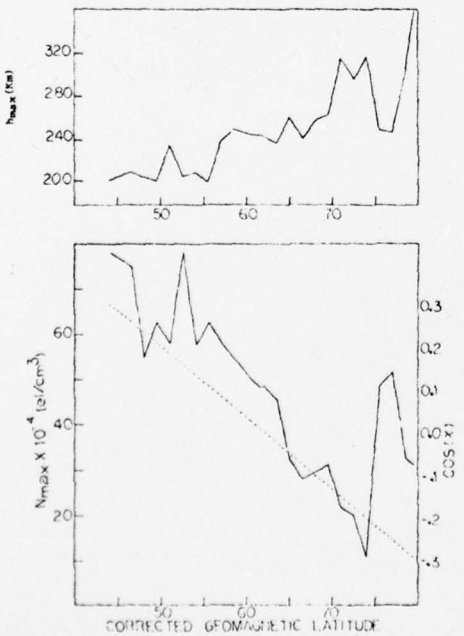

Fig. 2b. An individual quiet time Isis 2 pass near the noon meridian. One of the 15 passes that constitute Figure 2a, this orbital segment was traversed between 0006 and 0018 UT on December 9, 1971; $Kp = 1-$ to $2-$. The dashed line represents the cosine of the solar zenith angle.

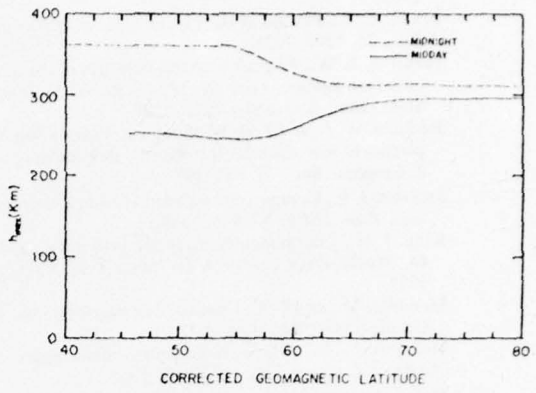

Fig. 3. Smoothed mean h_{max} curves near midnight (upper curve) and near midday (lower curve).

associated with it. The variation of hmF_2 and NmF_2 established here may therefore be taken to be representative of the magnetic latitude (CGL) dependence of these parameters along the noon-midnight meridian in midwinter under quiet magnetic conditions and moderate solar activity ($\bar{R} = 69$).

Figure 3 offers an interesting juxtaposition of the smoothed mean hmF_2 curves near noon and midnight. The 100-km diurnal difference usually attributed to the height of the mid-latitude F_2 peak [*Rishbeth and Garriott*, 1969] remains a good 'ball park' estimate when it is compared to the 107-km separation observed up to ~55° CGL in Figure 3. The 15-km diurnal separation found at the higher latitudes in Figure 3 should be viewed as nominal only, since the F_2 peak at these latitudes is characterized by wide fluctuations in altitude and density on both dayside and nightside.

The steady rise of hmF_2 and the accompanying steady fall in NmF_2 from ~55° to ~70° CGL near noon may simply reflect the solar zenith angle dependence of the magnitude and altitude of the production peak. Near midnight the lower (<55° CGL) and higher (>65° CGL) latitude plasma populations are likely to have been subjected to different E fields and neutral winds as well as to different loss and production processes, the former plasma having reached the midnight meridian by rotating around the duskside of the earth and the latter by convection across the polar cap. Hence the two plasma populations arrive to meet in the 55°–65° CGL range with different hmF_2 levels.

Acknowledgments. The author appreciates his discussions with Michael Mendillo on this work. It was supported by Air Force Geophysics Laboratory contracts F19628-75-C-0044 and F19628-78-C-0011 to Boston University.

The Editor thanks W. B. Hanson for his assistance in evaluating this brief report.

REFERENCES

Becker, W., The temperature of the *F* region deduced from electron number density profiles, *J. Geophys. Res.*, *72*, 2001, 1967.

Brinton, H. C., J. M. Grebowsky, and L. H. Brace, The high latitude winter *F*-region at 300 km: Thermal plasma observations from AE-C, *NASA Tech. Memo.*, *78101*, 1978.

Burch, J. L., Precipitation of low-energy electrons at high latitudes: Effects of interplanetary magnetic field and dipole tilt angle, *J. Geophys. Res.*, *77*, 6696, 1972.

Chacko, C. C., and M. Mendillo, Electron density enhancements in the *F* region beneath the magnetospheric cusp, *J. Geophys. Res.*, *82*, 4757, 1977.

Feinblum, D. A., and R. J. Horan, Hilion—A model of the high latitude ionospheric *F*2 layer and statistics of regular ionospheric

effects at Ft. Churchill, 1968, report, Bell Lab., Murray Hill, N. J., 1973.

Frank, L. A., Plasma in the earth's polar magnetosphere, *J. Geophys. Res.*, *76*, 5202, 1971.

Halcrow, B. W., *F*2 peak electron densities in the main trough region of the ionosphere, *Tech. Rep. PSU-IRI-IR-55*, Ionos. Res. Lab., Pa. State Univ., University Park, 1976.

Heikkila, W. J., and J. D. Winningham, Penetration of mangetosheath plasma to low altitudes through the dayside magnetospheric cusps, *J. Geophys. Res.*, *76*, 883, 1971.

Jackson, J. E., Comparison between topside and ground-based soundings, *Proc. IEEE*, *57*, 976, 1969.

King, J. H., Interplanetary magnetic field data, 1963–74, *Rep. UAG-46*, World Data Center A for Solar-Terr. Phys., Boulder, Colo., 1975.

Mendillo, M., and C. C. Chacko, The baselevel ionospheric trough, *J. Geophys. Res.*, *82*, 5129, 1977.

Muldrew, D. B., *F* layer ionization troughs deduced from Alouette data, *J. Geophys. Res.*, *70*, 2635, 1965.

National Climatic Center, Ionospheric data, *Rep. FA-351*, Asheville, N. C., 1973.

Pike, C. P., Equatorward shift of the polar *F* layer irregularity zone as a function of the *Kp* index, *J. Geophys. Res.*, *77*, 6911, 1972.

Rishbeth, H., and O. K. Garriott, *Introduction to Ionospheric Physics*, p. 177, Academic, New York, 1969.

Rycroft, M. J., and S. J. Burnell, Statistical analysis of movements of the ionospheric trough and the plasmapause, *J. Geophys. Res.*, *75*, 5600, 1970.

Thomas, J. O., J. Haselgrove, and A. R. Robbins, Tables of ionospheric electron density, Slough (England), Ser. B, no. 1, Radio Group, Cavendish Lab., Cambridge, England, 1957.

Titheridge, J. E., Ionospheric heating beneath the magnetospheric cleft, *J. Geophys. Res.*, *81*, 3221, 1976.

Tulunay, Y., and J. Sayers, Characteristics of the mid-latitude trough as determined by the electron density experiment on Ariel 3, *J. Atmos. Terr. Phys.*, *33*, 1737, 1971.

Yasuhara, F., S.-I. Akasofu, J. D. Winningham, and W. J. Heikkila, Equatorward shifts of the cleft during magnetospheric substorms as observed by Isis 1, *J. Geophys. Res.*, *78*, 7286, 1973.

(Received May 16, 1978;
revised June 30, 1978;
accepted July 7, 1978.)

REFERENCES

Ahmed, M., R.C. Sagalyn, P.J.L. Wildman and W.J. Burke, Topside ionosperic trough morphology: Occurrence frequency and diurnal, seasonal and altitude variations, J. Geophys. Res., 84, 489, 1979

Akasofu, S.-I., Polar and Magnetospheric substorms, D.Reidel, Dordrecht, Netherlands, 1968

Anger, C.D. and A.T.Y. Lui, A global view of the polar region on 18 December, 1971, Planet. Space Sci., 21, 873, 1973

Bates, H.F., A.E. Belon and R.D. Hunsucker, Aurora and poleward edge of the main ionospheric trough, J. Geophys. Res., 78, 648, 1973

Bendat, J.S. and A.G. Piersol, Random Data: Analysis and Measurement Procedures, Wiley-Interscience, New York, 1971

Brace, L.H. and R.F. Theis, The behavior of the plasmapause at mid-latitudes, J. Geophys. Res.,79, 1871, 1974

Brinton, H.C., J.M. Grebowsky and L.H. Brace, The high latitude winter F-region at 300 km: thermal plasma observations from AE-C, J. Geophys. Res., 83, 4767, 1978

Buchau, J., W.N. Hall, B.W. Reinisch and S. Smith, Remote ionospheric monitoring, AFGL-TR-78-0080, Air Force Geophysics Laboratory, Hanscom AFB, Bedford, MA 01731

Chacko, C.C, Magnetospheric Substorms and Auroral Particle Precipitation (thesis) Boston College, Chestnut Hill, MA 02167

Chacko, C.C. and M. Mendillo, High latitude ionospheric gradients and their relationships to auroral and magnetospheric boundaries, AFGL-TR-78-0092(i), Air Force Geophysics Laboratory, Hanscom AFB, Bedford, MA 01731

Eather, R.H. and S.B. Mende, Substorm effects in auroral spectra, J. Geophys. Res., 78, 7515, 1973

Eather, R.H., DMSP calibration, J. Geophys. Res., 84, 4134, 1979

Feinblum, D.A. and R.J. Horan, Helion - A model of the high latitude ionospheric F2 layer and statistics of regular ionospheric effects at Ft. Churchill, 1968, report, Bell Lab., Murray Hill, N.J., 1973

Feldstein, Y.I., S.I. Isaev and A.I. Lebedinsky, The phenomenology and morphology of aurorae, Annals of IQSY, 4, p311

Feldstein, Y.-I. and G.V. Starkov, Dynamics of auroral belt and polar geomagnetic disturbances, Planet. Space Sci., 15, 209, 1967

Halcrow, B.W., F2 peak electron densities in the main trough region of the ionsphere, Tech. Rep. PSU-IRL-IR-55, Ionos. Res. Lab., Pa. State Univ., University Park, 1976

Hoffman, R.A. and J.L. Burch, Electron precipitation patterns and substorm morphology, J. Geophys. Res., 78, 2867, 1973

Jones, R.A. and M.H. Rees, Time-dependent studies of the aurora-I. Ion density and Composition, Planet. Space Sci., 21, 537, 1973

Kamide, Y. and J.D. Winningham, A statistical study of the 'instantaneous' nightside auroral oval: the equatorward boundary of electron precipitation as observed by the ISIS 1 and 2 satellites, J. Geophys. Res., 82, 5573, 1977

Knudsen, W.C., Magnetospheric convection and the high latitude F-2 ionosphere, J. Geophys. Res., 79, 1046, 1974

Lui, A.T.Y. and C.D. Anger, A uniform belt of diffuse auroral emission seen by the ISIS-2 scanning photometer, Planet. Space Sci., 21, 799, 1973

Lui, A.T.Y., P. Perreault, S.-I. Akasofu and C.D. Anger, The diffuse aurora, Planet. Space Sci., 21, 857, 1973

Lui, A.T.Y., C.D. Anger and S.-I. Akasofu, The equatorward boundary of the diffuse aurora and auroral substorms as seen by the ISIS-2 auroral scanning photometer, J. Geophys. Res., 80, 3603, 1975a

Lui, A.T.Y., C.D. Anger, D. Venkatesan, W. Sawchuk and S.-I. Akasofu, The topology of the auroral oval as seen by the ISIS-2 scanning auroral photometer, J. Geophys. Res., 80, 1795, 1975b

Lui, A.T.Y., D. Venkatesan, C.D. Anger, S.-I. Akasofu, W.J. Heikkila, J.D. Winningham and J.R. Burrows, Simultaneous observations of particle precipitations and auroral emissions by the ISIS-2 satellite in the 19-24 MLT sector, J. Geophys. Res., 82, 2210, 1977

Mendillo, Michael and C. C. Chacko, The base level ionospheric trough, J. Geophys. Res., 82, 4757, 1977

Meng, C.-I., B.Mauk and C.E. McIlwain, Electron precipitation of evening diffuse aurora and its conjugate electron fluxes near the magnetospheric equator, J. Geophys. Res., 84, 2545, 1979

Mizera, P.F., D.R. Croley,Jr., F.A. Morse and A.L. Vampola, Electron fluxes and correlations with quiet-time auroral arcs, J. Geophys. Res., 80, 2129, 1975

Pike, C.P. and J.A. Whalen, Satellite observations of auroral substorms, J. Geophys. Res., 79, 985. 1974

Pike, C.P., Defense Meteorological Satellite Program Auroral Ionospheric Interpretation Guide, AFGL-TR-75-0191, Air Force Geophysics Laboratory, Hanscom AFB, Bedford, MA 01731

Rees, M.H., Auroral Ionization and excitation by incident energetic electrons, Planet. Space Sci., 11, 1209, 1963

Shepherd, G.G., F.W. Thirkettle and C.D. Anger, Topside optical view of the dayside cleft auroras, Planet. Space Sci., 24, 937, 1976

Tulunay, Y. and J. Sayers, Characteristics of the midlatitude trough as determined by the electron density experiment on Ariel III, J. Atmos. Terr. Phys., 33, 1737, 1971

Vondrak, R.R. and M.J. Baron, Radar measurements of the latitudinal variation of auroral ionization, Radio Sci., 11, 939, 1976

Wagner, R.A., A.L. Snyder and S.-I. Akasofu, The structure of the polar ionosphere during exceptionally quiet times, Planet. Space Sci., 21, 1911, 1973

Whitteker, J.H., The transient response of the topside ionosphere to precipitation, Planet. Space Sci., 25, 773, 1977